LASER SYNTHESIS AND PROCESSING OF COMPOSITE NANOSTRUCTURES

Mihaela Koleva [1,2], Anna Dikovska [1], Nikolay Nedyalkov[1],
Tsanislava Genova[1], Genoveva Atanasova[3]

[1]*Institute of Electronics, Bulgarian Academy of Sciences*
72 Tsarigradsko Chaussee Blvd., Sofia 1784, Bulgaria
[2]*South-West University "Neofit Rilski"*
66 Ivan Mihailov Str., Blagoevgrad, 2700, Bulgaria
[3]*Institute of General and Inorganic Chemistry*
Bulgarian Academy of Sciences, Acad. G. Bonchev St.
Bl. 11, Sofia 1113, Bulgaria
E-mail: mihaela_ek@swu.bg

Received 20 September 2023
Accepted 10 January 2024
DOI: 10.59957/jctm.v59.i4.2024.11

ABSTRACT

The present work reports the fabrication of porous composite ZnO/noble metal (Ag, Au) nanostructures using ps-pulsed laser deposition at atmospheric pressure. The PLD grown samples are ns-laser annealed, which led to a surface modification and formation of nanoparticles and NP's aggregates. The effect of laser annealing procedure on the morphology, structure and optical properties of composite nanostructures is studied. The experimental results indicate that the laser annealing changes the plasmon resonance absorption mostly in the silver-doped samples. The laser modification plays a key role in tuning the PL performance for all samples by different mechanisms. Along with the increase in UV emission, there is a corresponding decrease in the broadband defect emission with the laser modification of composite nanostructures. The plasmon resonance absorption contributes to the enhancement of photoluminescence band-edge UV emission of the silver doped samples, while the PL performance of nanostructured ZnO/Au samples is attributed to the surface-plasmon-mediated sequential transfer of defect energy from ZnO to Au and electron transfer from excited Au to ZnO.

Keywords: pulsed laser deposition, laser processing, nanocomposites, noble metals, surface plasmon resonance, photoluminescence.

INTRODUCTION

The pulsed laser deposition (PLD) is a well-established, versatile deposition technique with considerable advantages with respect to the other techniques. It is a clean, flexible and straightforward deposition scheme, compatible with different type of materials, which permits the deposition of uniform films with good adhesion and weak residual stress [1 - 3]. In the recent years, the open-air pulsed laser deposition technique (at atmospheric pressure) has been proven as a practical and inexpensive method for simple preparation of high-porosity nanostructures made up of nanoparticles. The laser ablation in open air results in nanoparticles and/or nanoparticle aggregates formation in the plasma plume realized via a fast condensation of the ablated material. Most studies reported the use of nanosecond pulsed laser sources in the ultraviolet region, but the PLD technique in the nanosecond range presents some drawbacks as low deposition rate [4, 5]. The studies employing femtosecond laser pulses have also been carried out. The motivation of these studies are potential advantages of the ultrafast laser ablation, such as non-thermal melting, highly energetic ablated species, and the absence of interaction between the incoming laser beam with the expanding plume, thus improving the properties and quality of the films.

The nanocomposites based on the embedded metal

nanoparticles in semiconductor matrices, where the role of plasmonic noble metals in the enhanced functions, are the objects of intensive studies for over the last years. These nanocomposite materials have important properties for applications depending on the kind of metal nanoparticles [6]. The efforts are focused on the improvement of performance of ZnO in combination with noble metals for applications in optoelectronic devices such as light emitting diodes [7]. Ag nanoparticles are interesting because of the position of the plasmon resonance. The LSPR wavelength maximum of small Ag nanoparticles with a diameter of 10 nm in air is around 420 nm, which allows several additional applications in comparison with similar Au nanoparticles, which have a maximum at around 530 nm [3]. The Ag peak at the wavelength at about 350 - 360 nm could correspond to quadrupole resonance [8, 9]. Quadrupole resonance is usually observed for nanostructures of larger size.

Zinc oxide (ZnO) has many attractive properties, as the high exciton binding energy, which makes it promising for creating ultraviolet LEDs, lasers, photosensors, piezoelectric and transparent electrodes, etc. [10, 11]. Zinc oxide is a wide band gap n-type semiconductor and hence it is attractive for optoelectronic device application in the ultraviolet (UV) wavelength range [12]. The large exciton binding energy can give a strong UV emission at room temperature. Apart from the near-band-edge emission (NBE) emission in the UV region, it also exhibits a deep-level emission (DLE) emission in the visible range, which is attributed to the intrinsic defects of ZnO [13]. The origin of DLE are intrinsic point defects including zinc vacancy (V_{Zn}), oxygen vacancy (V_O), zinc interstitials (Zn_i) and oxygen antisites (O_{Zn}) of ZnO [14, 15]. A particular intrinsic defect highly depends on the experimental conditions such as annealing temperature and environment.

The composite nanostructures usually demonstrate unique properties not observed in the separate materials. The plasmonic nanostructures of noble metals combined with semiconductors offer promising properties [6, 16, 17]. The overlap of the spectral range of the incident photon with absorbance wavelength of the ZnO semiconductor and the surface plasmon bands of the plasmonic metals provides a useful tool to predict the enhancement in optical and electrical properties of hybrid semiconductor-noble metal nanostructures.

Pulsed laser ablation is a successful method to synthesize ZnO NPs with controlled luminescence properties, thus increasing their application in lighting technologies [16, 18]. Pulse duration is a crucial parameter to determine the size and the optical properties of ZnO NPs [19]. The influence of pulse duration on the morphology and structure of the produced NPs is not well clarified, due to the lack of systematic study on a variety of materials.

In this work, we report on the effectiveness of ultrashort-pulsed laser deposition of composite ZnO/noble metal (Ag, Au) nanostructures in the atmospheric pressure, using picosecond pulses, as a continuation of our previous research on ns-PLD of ZnO/noble metal (Ag) in open air [16]. We investigate the influence of ns-laser annealing on the properties of the resulting films. The influence of the composition and morphology formed on the optical properties of produced composites is studied.

EXPERIMENTAL

Picosecond Nd:YAG laser (t = 10 ps) operating at a wavelength of 1064 nm with a pulse repetition rate of 1 kHz is used to deposit composite layers on SiO_2 (001) substrates. The deposition is performed for 2 min at a fluence of 0.5 J cm^{-2} at room temperature in the atmospheric pressure (open air). The target to substrate distance is 5 mm. Pulsed laser deposition in air is a quite inefficient process. When the target-substrate distance is larger than 5 mm, the material deposited on the substrate is barely observed. The ablated particles are scattered due to collisions with the ambient gas at atmospheric pressure, which results in a low deposition rate and, as a consequence, a negligible coverage of the substrate surface.

The nanosecond laser annealing of deposited samples is performed by nanosecond Nd:YAG laser system at the wavelength of 355 nm. The laser fluence is established at 0.7 J cm^{-2}. The samples are modified in the ambient pressure at 1 pulse.

The samples are obtained applying two deposition schemes. A schematic representation of the mosaic target configurations for laser ablation of ZnO partly covered by metal slice of Ag or Au is presented on Fig. 1 and the corresponding types of targets are shown in Table 1. Sample ZnO/Au-1 is deposited according to Scheme 1, i.e. the metal plate (Au) is located across the center of

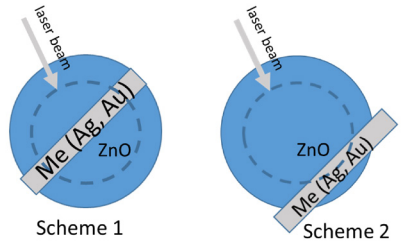


Fig. 1. Schematic representation of the composite target configurations for laser ablation of ZnO covered by metal slice of Ag or Au located: 1 - in the center, 2 - in the periphery.

Table 1. The types of composite targets according to the configurations in Fig. 1. The ZnO target is covered by metal slice of Ag or Au located: scheme 1 - in the center, scheme 2 - in the periphery.

	SCHEME 1	SCHEME 2
TARGET	ZnO/Au-1	ZnO/Au-2
	ZnO/Ag-1	ZnO/Ag-2
		ZnO/Ag-3 low speed of the target rotation

Table 2. Calculated elemental concentrations from XPS spectra of the ps-laser grown ZnO/noble metal (Ag, Au) composite samples.

Elements / Samples	Zn	Ag	Zn/Ag	Ag/Zn
ZnO/Ag-1	55.9	44.0	1.3	0.8
ZnO/Ag-2	79.0	20.9	3.8	0.3
ZnO/Ag-3	73.9	26.0	2.8	0.4
Elements / Samples	Zn	Au	Zn/Au	Au/Zn
ZnO/Au-1	88.4	11.5	7.7	0.1
ZnO/Au-2	94.3	5.6	16.7	0.1

the ZnO target. Sample ZnO/Au-2 is deposited according to Scheme 2, i.e. the metal plate (Au) is located at the periphery of the ZnO target. During ablation, the composite target is rotated and the laser beam scan across the target surface is marked in the dashed curve. The silver doped samples are obtained similarly. Sample ZnO/Ag-1 is deposited according to Scheme 1, i.e. the metal plate (Ag) is located across the center of the ZnO target. Sample ZnO/Ag-2 was deposited according to Scheme 2, i.e. the metal plate (Ag) is located at the periphery of the ZnO target. One additional ZnO/Ag-3 sample is also deposited according to Scheme 2, but with a lower speed of the target rotation. Layers with different concentrations of ZnO and Au/Ag are obtained because of different deposition Schemes (Table 2).

The rotation of the mosaic targets is using for uniform ablation. The effect of target rotation rate on the properties of PLD grown ZnO/Ag nanocomposite is investigated. The rotation rate of the target for the ZnO/Au samples and ZnO/Ag-1, ZnO/Ag-2 samples is 3000 rpm, while the speed of the target rotation of ZnO/Ag-3 sample is fixed at 1500 rpm.

The morphology of the fabricated nanostructures is observed by scanning electron microscopy (SEM) using a LYRA I XMU system (Tescan). The chemical surface composition of the samples are examined by X-ray photoelectron spectroscopy (XPS) by means of an AXIS Supra electron spectrometer (Kratos Analytical Ltd.). The UV-Vis transmission spectra are recorded in the spectral range of 210 - 850 nm by an HR 4000 UV-Vis spectrometer (Ocean Optics).The photoluminescence (PL) measurements of the samples are conducted on a FluoroLog 3 spectrofluorometer (HORIBA Jobin Yvon) with 320 nm excitation light.

RESULTS AND DISCUSSION

This study is focused on fabricating ZnO/noble metal (Ag, Au) nanostructures by picosecond pulsed laser deposition in open air and investigating the effect of a nanosecond laser annealing procedure on the morphology and optical properties of composite nanostructures. A porous structures composed by wires and arranged particles are fabricated. Fig. 2 shows SEM images of the morphology of the samples deposited after ablation of a ZnO/noble metal target in open air and the samples after the laser annealing. During the deposition process the wire structures with lengths of several microns are formed on the substrate (Fig. 2a, d and g). SEM images show that the formation of nanostructures is influenced by the speed of the target rotation during the picosecond laser deposition. The laser annealing applied leads to the formation of a structure consisting of randomly distributed nanoparticle aggregates and free nanoparticles with mean diameters

up to 180 nm. The higher magnification of SEM images of the samples reveals the presence of free nanoparticles (inset in Fig. 2b). After the laser annealing procedures, the samples decompose into nanowires, nanochains, or nanoparticles. Changes occur in the size of the NPs and their interconnections. The morphology of all annealed doped samples greatly differs from the nanostructures produced by nanosecond PLD from mosaic targets previously studied [17]. Sample ZnO/Ag-3 demonstrates the most pronounced differences in morphology before and after the laser annealing, as well as a noticeable difference between the center and the periphery of the annealed spot. Which is due to a different composition distribution of ZnO and silver in the deposited layer, compared to sample ZnO/Ag-2. The nanoparticles form aggregates in the center of ZnO/Ag-3 sample and a wide NPs size distribution is observed.

The high-resolution XPS analyses of the nanostructures produced by PLD in open air are carried out in order to obtain information on their surface compositions and chemical states. The XPS spectra of the samples before the laser annealing are presented on

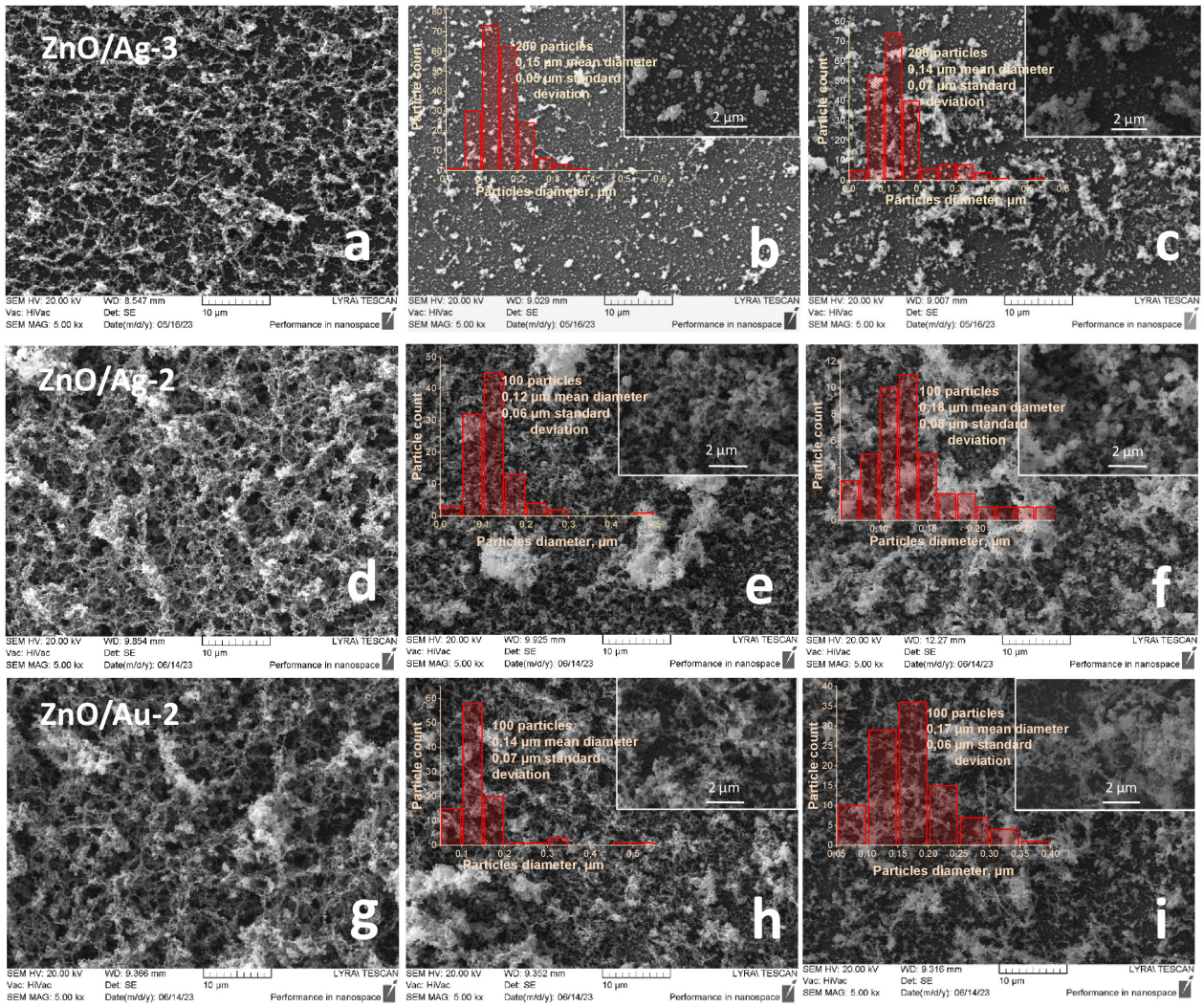


Fig. 2. SEM images of composite nanostructures before the laser annealing (a, d, g), after the laser annealing in the periphery of the spot (b,e h) and after the laser annealing in the center of the spot (c, f, i). The upper, central, and lower images refer to samples: ZnO/Ag-3, ZnO/Ag-2 and ZnO/Au-2, respectively. The insets show the magnified images and the histograms of the particles size distribution obtained from the scanning electron micrographs.

Fig. 3. The $Zn2p_{3/2}$ and $Zn2p_{1/2}$ peaks for ZnO sample are located at 1022.1 eV and 1045.2 eV, respectively, with spin-orbit splitting of 23.1 eV (Fig. 3a). The spin-orbit splitting, the binding energy positions and the width of the Zn2p peaks are in a good agreement with the oxidation state of Zn^{2+} in ZnO [20]. The Au4d and Ag3d XPS spectra from the surface of the nanocomposite samples are presented on Fig. 3b. High resolution spectrum of Au4d shows doublet components arising at binding energies of 334.0 eV and 352.9 eV and assigned to $Au4d_{5/2}$ and $Au\ 4d_{3/2}$ respectively (Fig. 3b). The peaks can be attributed to metallic gold and are in a good agreement with the XPS data reported in the literature [21]. The peaks corresponding to the $Ag3d_{3/2}$ and $Ag3d_{5/2}$ states of metallic silver are observed at 373.5 eV and 367.7 eV. As observed for other Ag–ZnO composites the binding energy of the Ag3d states is shifted to lower values when compared to bulk Ag [22]. This effect is often ascribed to the fact that Ag and ZnO adjust their Fermi level upon contact resulting in a partial oxidation of Ag [23].

The calculated elemental composition and relative concentrations from XPS spectra of the samples are presented in Table 2. Sample ZnO/Ag-1 demonstrates a significant difference in the concentrations compared to samples ZnO/Ag-2 and ZnO/Ag-3. While samples ZnO/Ag-2 and ZnO/Ag-3 have similar concentrations of the elements and the speed of target rotation have not a big influence on the composition. The gold-doped samples also demonstrate differences in the concentrations for the two types of samples, produced at different target schemes during the depositions.

The UV-Vis spectroscopy confirmed formation of silver nanoparticles in the composite samples. Fig. 4b shows the changes in optical absorption after the laser annealing in ZnO/Ag samples. The resonance absorption appears at the wavelength of 360 nm for the samples ZnO/Ag-2 and ZnO/Ag-3 doped with silver before the annealing. The sample ZnO/Ag-1 demonstrates mainly the absorption edge of ZnO before the annealing and appearance of plasmon resonance absorption after the annealing at 360 nm. The laser modification causes the appearance of the new resonance absorption band, which is related to the size of nanoparticles. It is well defined for sample ZnO/Ag-3. An additional dip in transmission spectrum comes at around 480 nm, which probably corresponds to the surface plasmon resonance in the small silver particles. This sample is characterized by wide size distribution of nanoparticles, where small and large NPs could be observed (Fig. 2c). The peak at the 360 nm could correspond to quadrupole resonance [24]. Quadrupole resonance usually is observed for nanostructures of larger size or in hexagonally shaped nanoparticles. However, the Mie theory could not directly indicate that this is a peak associated with quadrupole resonance, because its nature is not fully understood [24].

The photoluminescence spectra display near-band-edge emission (NBE) peak in ultraviolet (UV) region at around 381 nm and the deep-level emission (DLE) peak centered at around 540 nm. The UV emission band is related to a near band-edge transition of ZnO, namely the recombination of the free excitons [25, 26].

An examination of the photoluminescence

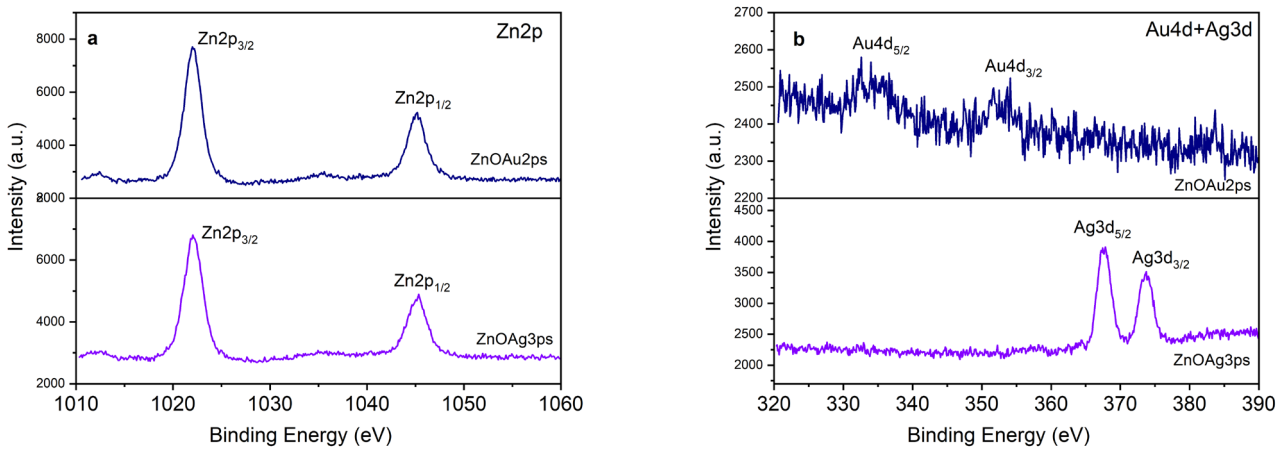


Fig.3. High resolution (a) Zn2p, (b) Au4d and Ag3d XPS spectra of nanocomposites ZnO/Au-2 and ZnO/Ag-3.

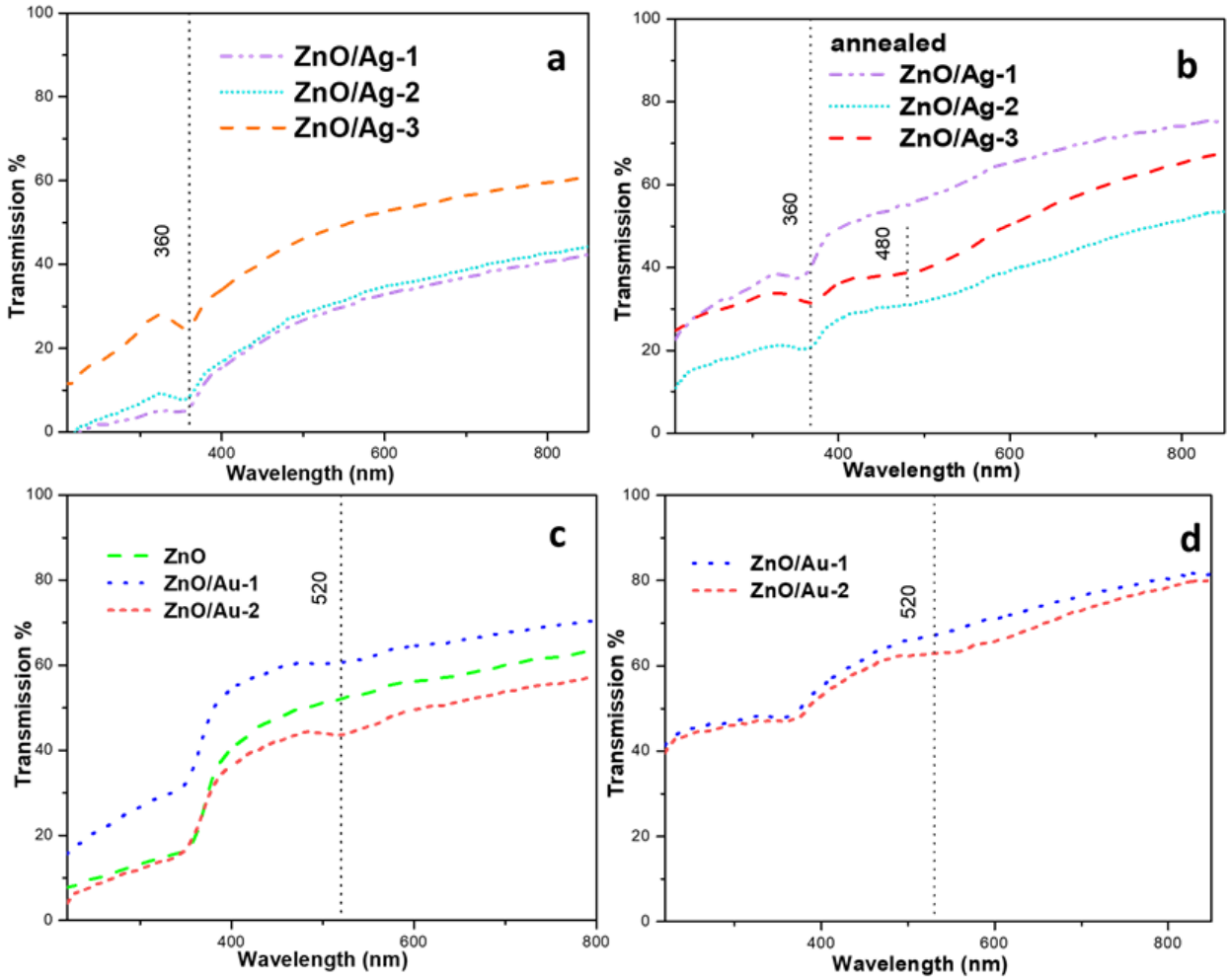


Fig. 4. Transmission spectrum of laser grown (a, c) and laser annealed (b, d) nanostructures of ZnO/Ag and ZnO/Au.

spectra of ZnO/noble metal nanocomposites at the selected excitation wavelength of 320 nm showed the enhancement of the near-band-edge UV emission and suppression of deep-level emission by laser annealing compared to that before annealing (Fig. 5). The ZnO deep-level emission appears in the green and yellow regions of the visible spectrum. The relative PL intensity ratio between the UV emission and deep level emission can be used to characterize the crystallization. The larger intensity ratio indicates better crystallization, i.e. less deep level defects. The intensity ratio of the near-band-edge emission to deep-level emission increases after the laser processing. It is highly pronounced for sample ZnO/Ag-1, where the resonance absorption appears after the laser annealing.

Surface plasmon resonance properties affect the UV band-gap emission of the silver doped samples, while the change in the emission properties of the gold doped samples is due obviously to the other mechanisms. The differences in the SPR properties of the gold-doped nanostructures before and after the laser processing are not essential. The resonant absorption of gold NPs is located at 520 nm, i.e. away from the UV band of the PL emission of ZnO. The UV absorption band of silver doped samples is centered at 360 nm, which is closer to the UV PL emission (380 nm). Most probably, the PL band emission of the gold-doped samples is enhanced through the transfer of defect emission based on the energy match between the defect emission of ZnO and the surface-plasmon excitation of Au nanoparticles in the hybrid system consisting of ZnO and Au NPs [27].

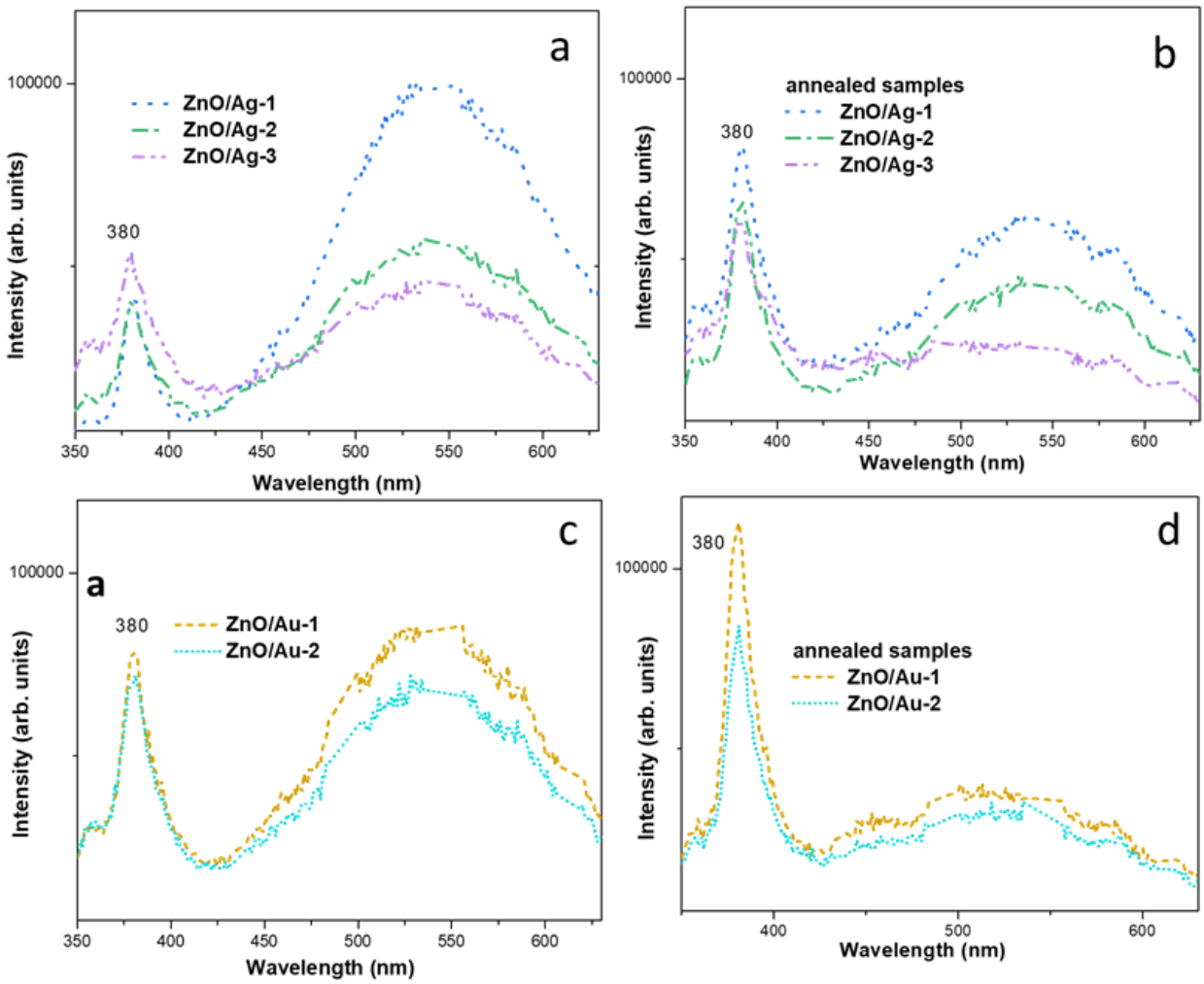


Fig. 5. Photoluminescence spectra of composite nanostructures: (a) ZnO/Ag before the annealing, (b) ZnO/Ag after the laser annealing, (c) ZnO/Au before the annealing, (d) ZnO/Au after the laser annealing.

CONCLUSIONS

In this study was found that highly porous ZnO/noble metal (Ag, Au) thin films can be prepared by ps-PLD in open air. The configuration of the mosaic target leads to variations in the compositions, but the target rotation speed does not affect considerably the composition of the samples. Nevertheless, the speed of the target rotation reflects on the optical properties of the samples, and it is associated with the samples morphology. The laser processing have a weak influence on the morphology and plasmon resonance absorption of the produced ZnO/Au nanostructures. The silver-doped samples exhibit pronounced change in the morphology and SPR properties, especially the sample ZnO/Ag-3. Sample ZnO/Ag-1 does not demonstrate the SPR properties before the annealing but exhibits significant amplification of the UV PL signal after the laser modification, associated with the appearance of resonant absorption at 360 nm. The control of PL properties of the produced nanocomposites relies on tailoring the material properties through a suitable choice of the laser parameters and conditions for synthesis and processing. The results obtained demonstrate different mechanisms for tuning the PL performance of the composites. The silver-doped ZnO samples demonstrate a surface-plasmon-enhanced UV photoluminescence, while the proposed possible mechanism for the enhanced band emission of gold-doped samples is a sequential transfer of defect energy from ZnO to Au and electron transfer from excited Au to ZnO.

Acknowledgements

The authors acknowledge the financial support of the BNSF under the project KP-06-N37/20 entitled "Formation and physical properties of composite nanostructures of metal oxides and noble metals".

REFERENCES

1. D.B. Chrisey, G.K. Hubler, Pulsed Laser Deposition of Thin Films, John Wiley and Sons, New York, USA, 1994.
2. A.J. Haider, T. Alawsi, M.J. Haider, B.A. Taha, H.A. Marhoon, A comprehensive review on pulsed laser deposition technique to effective nanostructure production: Trends and challenges, Opt. Quantum Electron., 54, 2022, 488.
3. A. Perrone, A.P. Caricato, A. Luches, M. Dinescu, C. Ghica, V. Sandu, A. Andrei, Boron carbonitride films deposited by pulsed laser ablation, Appl. Surf. Sci., 133, 1998, 239-242.
4. G. García Guillén, M.I. Mendivil Palma, B. Krishnan, D. Avellaneda, G.A. Castillo, T.K. Das Roy, S. Shaji, Structure and morphologies of ZnO nanoparticles synthesized by pulsed laser ablation in liquid: Effects of temperature and energy fluence, Materials Chemistry and Physics, 162, 2015, 561-570.
5. D. Dellasega, V. Russo, A. Pezzoli, C. Conti, N. Lecis, E. Besozzi, M. Beghi, C.E. Bottani, M. Passoni, Boron filmsproduced by high energy Pulsed Laser Deposition, Mater. Des., 134, 2017, 35-43.
6. M.E. Koleva, A.Og. Dikovska, N.N. Nedyalkov, P.A. Atanasov, I.A. Bliznakova, Enhancement of ZnO photoluminescence by laser nanostructuring of Ag underlayer, Applied Surface Science, 258, 23, 2012, 9181-9185.
7. O. Lupan, T. Pauporte, B. Viana, Low-Voltage UV-Electroluminescence from ZnO-Nanowire Array/p-GaN Light-Emitting Diodes, Adv. Mater. 22, 30, 2010, 3298-3302.
8. H.Oh,A. Pyatenko, M. Lee , Laser dewetting behaviors of Ag and Au thin films on glass and Si substrates: Experiments and theoretical considerations, Appl. Surf. Sci., 475, 2019, 740-747.
9. U. Kreibig, P. Zacharias, Surface plasma resonances in small spherical silver and gold particles, Z. Physik, 231, 1970, 128-143.
10. U. Ozgur, Ya.I. Alivov, C. Liu, A Teke, M.A. Reshchikov, S. Dogan, V. Avrutin, S.-J. Cho, H. Morkoc, A comprehensive review of ZnO materials and devices J. Appl. Phys., 98, 4, 2005, 041301.
11. C.R. Gorla, N.W. Emanetoglu, S. Liang, W.E. Mayo, Y. Lu, M. Wraback, H. Shen, Structural, optical, and surface acoustic wave properties of epitaxial ZnO films grown on (01$\bar{1}$2) sapphire by metalorganic chemical vapor deposition J. Appl. Phys. 85, 5, 1999, 2595.
12. V.A. Fonoberov, Kh.A. Alim, A.A., Balandin, F. Xiu, J. Liu, Photoluminescence investigation of the carrier recombination processes in ZnO quantum dots and nanocrystals, Phys. Rev. B, 73, 2006, 165317.
13. N.O. Korsunska, L.V. Borkovska, B.M. Bulakh, L.Yu. Khomenkova, V.I. Kushnirenko, I.V. Markevich, The influence of defect drift in external electric field on green luminescence of ZnO single crystals, J. Lumin, 102-103, 2003, 733-736.
14. A. Janotti and Ch. G. Van de Walle, Native point defects in ZnO, Phys. Rev. B, 76, 2007, 165202.
15. B.X. Lin, Z.-X. Fu, Y.-B. Jia, Green luminescent center in undoped zinc oxide films deposited on silicon substrates, Appl. Phys. Lett., 79, 7, 2001, 943-945.
16. M.E. Koleva, A.O. Dikovska , N.N. Nedyalkov and D. Karashanova, Effect of laser annealing on the properties of Ag/ZnO nanostructures, J. Physics: Conference Series, 2240, 2022, 012008.
17. M.E. Koleva, N.N. Nedyalkov, N. Fukata, W. Jevasuwan, S. Amoruso, T. Koutzarova, G. V. Avdeev, B. Georgieva, D. Karashanova, Laser-assisted approach for synthesis of plasmonic Ag/ZnO nanostructures, Superlattices and Microstructures, 109, 2017, 886-896.
18. R. Zamiri, A. Zakaria, H. Abbastabar Ahangar, M. Darroudi, A. Khorsan Zak, and G.P.C. Drummen, Aqueous starch as a stabilizer in zinc oxide nanoparticle synthesis via laser ablation, Journal of Alloys and Compounds 516, 2012, 41-48.
19. B. Liu, Zh. Hu, Y. Che, A. Allenic, K. Sun, X. Pan, Growth of ZnO nanoparticles and nanorods with ultrafast pulsed laser deposition, Appl. Phys. A, 93 2008, 813-818.
20. M.C. Biesinger, L.W.M. Lau, A.R. Gerson, R. St, C. Smart, Resolving surface chemical states in XPS analysis of first row transition metals, oxides and

hydroxides: Sc, Ti, V, Cu and Zn, Appl. Surf. Sci., 257, 2010, 887-898.
21. Y. Xu, B. Yao, Y.F. Li, Z.H. Ding, J.C. Li, H.Z. Wang, Z.Z. Zhang, L.G. Zhang, H.F. Zhao, D.Z. Shen, Chemical states of gold doped in ZnO films and its effect on electrical and optical properties. J Alloys Compd., 585, 2014, 479-484.
22. J.F. Moudler, W.F. Stickle, P.E. Sobol, K.D. Bomben, Handbook of X-ray photoelectron spectroscopy, Perkin-Elmer, Eden Prairie, MN, 1992.
23. Y. Zheng, L. Zheng, Y. Zhan, X. Lin, Q. Zheng, K. Wei, Ag/ZnO heterostructure nanocrystals: synthesis, characterization, and photocatalysis, Inorg Chem 46, 17, 2007, 6980.
24. K.L. Kelly, E. Coronado, L.L. Zhao, G.C. Schatz, The Optical Properties of Metal Nanoparticles: The Influence of Size, Shape, and Dielectric Environment, J Phys Chem B., 107, 2003, 668-677.
25. Y. Chen, N.T. Tuan, Y. Segawa, H.Ko, S. Hong, T. Yao, Stimulated emission and optical gain in ZnO epilayers grown by plasma-assisted molecular-beam epitaxy with buffers, Appl. Phys. Lett., 78, 2001, 1469.
26. W.I. Park, S.J. An, G.C. Yi, H.M. Jang, Metal-organic vapor phase epitaxial growth of high-quality ZnO films on Al_2O_3 (00-11), Journal of Materials Research 16, 5, 2001, 1358-1362.
27. S.T. Kochuveedu, J.H. Oh, Y.R. Do, D.H. Kim, Surface-plasmon-enhanced band emission of ZnO nanoflowers decorated with Au nanoparticles, Chemistry, 18, 24, 2012, 7467-72.